Structural and Magnetic Properties of the Rapid Cooled Alloys: $Fe_{60}Co_{10}Y_{5+x}Zr_{5-x}B_{20}$ (Where: x = 0 or 2)

MARCIN NABIALEK[1]*, BARTLOMIEJ JEZ[1], KINGA JEZ[1], KATARZYNA BLOCH[1]

[1]Institute of Physics, Faculty of Production Engineering and Materials Technology, Czestochowa University of Technology, 19 Armii Krajowej Str., 42-200 Czêstochowa, Poland

This article presents the results of tests on high-temperature alloys, produced on the basis of the FeCoB matrix. The nanocrystalline material was produced in a single-step process of rapid cooling of liquid alloy that was injected into a copper mould. Alloy samples were obtained in the form of 10mm x 5mm x 0.5mm tiles. Studies of the structure of the manufactured alloys were undertaken using Bruker X-ray analysis equipment (featuring a CuKa lamp). The magnetic polarization of saturation was measured, as a function of temperature, using a Faraday magnetic balance; the measurements ranged from room temperature up to 850K. Through numerical analysis of the curves, the Curie temperature of the investigated alloys was determined. Using a vibration magnetometer, static magnetic hysteresis loops were measured. The magnetization of saturation of the tested alloys was greater than 1 T, while the coercive field values were 400 and 16600 A/m. The stiffness parameter of the spin wave D_{spf} was determined.

Keywords: FeCoB matrix, nanocristalline material, Bruker K-ray

Soft magnetic materials are representatives of a wide range of functional materials. They are characterized, among other features, by a low value of coercive field and a high magnetization of saturation [1-3]. Soft magnetic properties are exhibited, among others, by rapidly-cooled FeCoB-based alloys [4-6]. Amorphous and nanocrystalline alloys with a high iron content can be an alternative material for FeSi sheets in the production of low-loss transformer cores [7]. The most well-known methods of producing quick-cooled alloys involve the rapid cooling of the liquid alloy. A sufficiently high cooling rate allows the material to solidify before it has the opportunity to crystallize. Alloys with amorphous and nanocrystalline structure usually have better strength and magnetic properties compared with crystalline alloys featuring the same chemical composition [8-10].

Melt-spinning is a well-known method for the production of rapidly-cooled alloys. The method involving the casting of liquid alloy onto a rotating copper cylinder facilitates the production of thin strips of alloy; the resulting alloy has a thickness of several tens of mm). The limited applicability of these materials, along with their unique properties, has mobilized scientists to seek new high-speed alloys and new methods for their production. In this way, a new group was created: massive amorphous materials [10, 11]. Methods for producing massive amorphous materials feature a cooling rate in the range of 10^{-1} to 10^{3} K/s, while unidirectional cooling on a rotating cylinder reaches speeds of the order of 10^{6} K/s. The potential for the creation of an amorphous structure is not only associated with the cooling rate; the slowdown of the crystallization process is possible by limiting the diffusion of atoms within the volume of the alloy over further distances. This can be achieved by appropriate selection of the chemical composition. For this purpose, it is necessary to ensure high melt viscosity, low melting point of the alloy and correspondingly large differences in the atomic radius length of the main components [12,13]. The application of these criteria increases the probability of obtaining an amorphous structure for larger size alloy samples, considering previously researches [14-25].

Volume rapidly-cooled alloys are an interesting research subject. It is notable that there are significant differences in the structure of the alloys obtained, and their magnetic properties, for the same chemical compositions produced by methods with different cooling rates. The cooling rate affects the degree of disorder of the atoms within the volume of the samples produced. During the production of massive amorphous materials, a certain degree of relaxation of their structure occurs. Variation in the cooling rate of the liquid alloy affects the type and quantity of defects present in the amorphous structure. For amorphous materials, there are defects in the form of free volumes and pseudo-lockable dipoles; the counterparts in crystalline materials are vacancies and linear defects. The type and number of defects affect, among other properties, the method of material magnetization [26-28]. Grains of crystalline phases, distributed in the amorphous matrix, can exert a significant influence on the magnetic properties of the high temperature alloys. Materials of this type are often produced by heat treatment of amorphous precursors. However, it is possible to produce nanocrystalline material in a single-step process, concurrent with the rapid-cooling of the liquid alloy. Appropriate selection of the chemical composition and cooling rate allows the partial crystallization of the alloy during its solidification. The creation of grains of the crystalline phase, with dimensions not exceeding 100 nm, within the amorphous matrix promotes the creation of good soft magnetic properties [29].

The aim of this work was to produce rapidly-cooled alloys with the chemical composition $Fe_{60}Co_{10}Y_{5+x}Zr_{5-x}B_{20}$ (where: x = 0 or 2). This was to be achieved through the injection of the liquid alloy into a copper mould. The work involved investigations into the structure and magnetic properties of the alloys.

Experimental part

Material and methods

Each respective rapidly-cooled alloy was prepared from the starting polycrystalline alloy: $Fe_{60}Co_{10}Y_{5+x}Zr_{5-x}B_{20}$ (where: x = 0 or 2). Elements with a purity exceeding 99.99% of the batch material were weighed out to the

*email: nmarcell@wp.pl

nearest 0.001 gram. A polycrystalline ingot was made using a plasma arc under a protective atmosphere of argon. Repeated melting of the batch ensured thorough mixing of the alloy components. Prior to melting the investigated alloys, an ingot of pure titanium was melted each time. The absorption of dirt and oxygen particles remaining in the working chamber ensured a higher degree of purity of the ingot. The high-melt alloy was produced through the injection of the liquid alloy into the copper mould. The ingot was placed in a quartz capillary, which, in turn, was installed within a copper coil - in such a way that the ingot was located in the centre of the coil. The batch was inductively melted. After melting, the batch was forced through a hole in the capillary, into the cylindrical copper mould. The alloy was obtained in the form of 10mm x 5mm x 0.5mm tiles. The whole process took place under a protective atmosphere of argon.

The structure of the obtained samples was examined using X-ray diffraction. The test was conducted on powder samples. The X-ray diffractometer was equipped with a CuKa lamp. The test was carried out for an angle of 2-theta over the range from 30° to 100°. The magnetic properties of the samples were tested using a Faraday magnetic balance and a vibration magnetometer. The sizes of the crystalline phase grains were estimated using the Scherrer formula: (1):

$$D=(\lambda*K)/2\beta_0 cos\Theta \quad (1)$$

K – shape coefficient (K = 0.91)

λ– characteristic wavelength

B_0 –half width in the middle of the intensity of the peak (the background included in the analysis)

Θ-Bragg angle

The stiffness parameter of the spin-wave, D_{spf}, was determined for the tested alloy samples. This parameter was determined using the following expression:

$$b = 3,54 g\mu_0\mu_B \left(\frac{1}{4\pi D_{spf}}\right)^{3/2} kT(g\mu_B)^{1/2} \quad (2)$$

where: b - slope of a linear fit corresponding to the thermally induced suppression of spin waves by a high intensity magnetic field, μ_0 - magnetic vacuum permeability, k - Boltzmann constant, μ_B - Bohr magneton, g - a magnetometric coefficient.

Results and discussions

In figure 1, X-ray diffractograms are shown, which were measured for alloy samples with the chemical composition $Fe_{60}Co_{10}Y_{5+x}Zr_{5-x}B_{20}$ in the post-solidification state. The diffractogram for the $Fe_{60}Co_{10}Y_5Zr_5B_{20}$ alloy shows a wide maximum in the angle of 2-theta between 40° - 50°. This maximum indicates the presence of a disordered phase within the volume of the sample being tested. In addition, narrow peaks, derived from crystalline phases, are visible on the diffractogram. The diffractogram in figure 1b consists of a larger number of narrow peaks. An outline of a broad maximum is visible and this is related to the presence of the amorphous phase within the volume of the sample under test. The type of phases formed within the melt volume was identified using the Match! program.

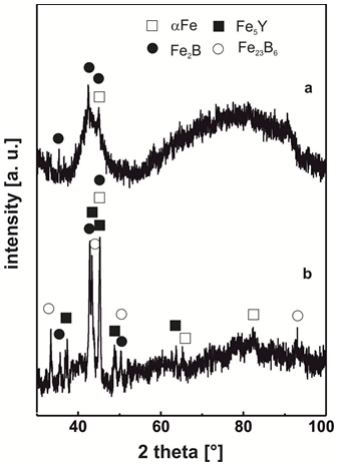

Fig.1. X-ray diffractograms measured for alloys: a) $Fe_{60}Co_{10}Y_5Zr_5B_{20}$, b) $Fe_{60}Co_{10}Y_7Zr_3B_{20}$.

Using the Scherrer formula, crystallite sizes were determined; data are given in table 1.

The soft magnetic phasesaFe and Fe_2B were identified in the $Fe_{60}Co_{10}Y_5Zr_5B_{20}$ alloy. In the case of the alloy with the higher content of yttrium, the phase described as magnetically semi-hard Fe_5Y and magnetically soft $Fe_{23}B_6$ were additionally identified. The estimated dimensions of the identified crystalline phases did not exceed the 100nm criterion dimension which classifies the materials produced as nanocrystalline.

Figure 2 presents thermomagnetic curves for samples of the investigated alloys.

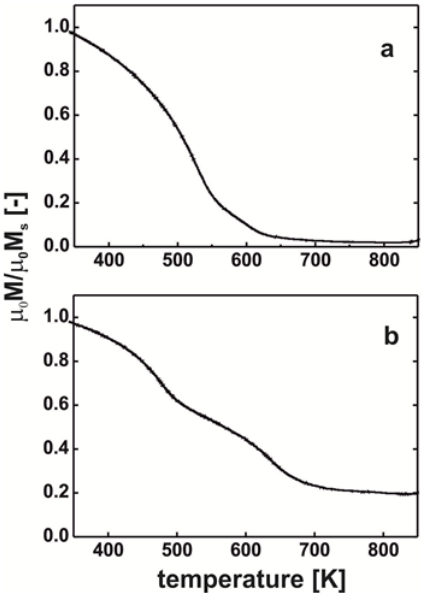

Fig.2. Measured magnetization saturation curves, as a function of temperature, for alloys: a) $Fe_{60}Co_{10}Y_5Zr_5B_{20}$, b) $Fe_{60}Co_{10}Y_7Zr_3B_{20}$.

Measurement of magnetization, as a function of temperature, was carried out over the range from room temperature to 850K with constant magnetic field strength. On the thermomagnetic curve for the alloy $Fe_{60}Co_{10}Y_5Zr_5B_{20}$, one curve associated with the transition of the magnetic phase from the ferromagnetic to paramagnetic state is observed. This phase is an amorphous matrix. From the course of the magnetization curve, it can be concluded that there are no other magnetic phases (over the tested temperature range) in the melt volume. In the case ofthe $Fe_{60}Co_{10}Y_7Zr_3B_{20}$ alloy, the course of the magnetization curve(as a function of temperature) is different. There are

Table 1

ESTIMATED CRYSTALLITE SIZES, GENERATED DURING THE RAPID COOLING OF THE LIQUID ALLOY $Fe_{60}Co_{10}Y_{5+x}Zr_{5-x}B_{20}$.

Crystalline Phase / Alloy	αFe [nm]	Fe_2B[nm]	Fe_5Y [nm]	$Fe_{23}B_6$ [nm]
$Fe_{60}Co_{10}Y_5Zr_5B_{20}$	13.2	18.5	-	-
$Fe_{60}Co_{10}Y_7Zr_3B_{20}$	16.2	21.3	23.9	18.9

two inflections from the change in state of magnetic phases from ferromagnetism to paramagnetism. Gentle transitions suggest the presence of two magnetic phases with different Curie temperatures. The value of magnetization at the temperature above the second inflection confirms significant presence of a crystalline phase with a Curie temperature exceeding 850K. According to the diffractogram (Figure 1b), these should be Fe_5Y and Fe_2B phases, which transition to a paramagnetic state at temperatures above 850K. Figure 3 presents magnetic saturation polarization curves, which were subjected to numerical analysis. Determination of the Curie temperature was possible due to the use of a critical factor: b =0.36for ferromagnetics that meet Heisenberg's assumptions.

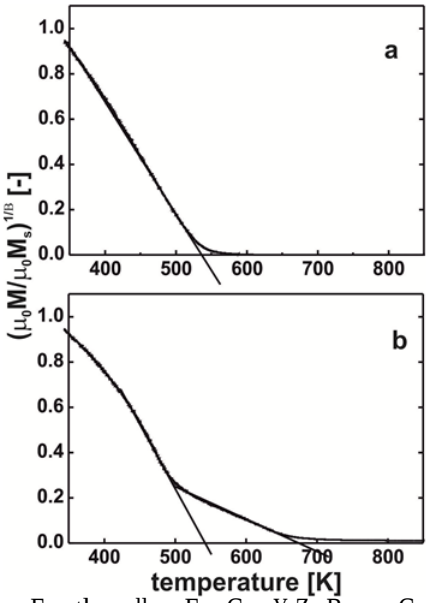

Fig.3. Determined Curie temperature for alloys: a) $Fe_{60}Co_{10}Y_5Zr_5B_{20}$, b) $Fe_{60}Co_{10}Y_7Zr_3B_{20}$.

For the alloy $Fe_{60}Co_{10}Y_5Zr_5B_{20}$, a Curie temperature of 535K was determined. It should be assumed that this is related to the amorphous phase identified on the basis of the diffractogram (fig. 1a). Two Curie temperatures were determined for the $Fe_{60}Co_{10}Y_7Zr_3B_{20}$ alloy. The first of them, 543K, is associated with the presence of an amorphous matrix within the volume of the alloy. The higher Curie temperature of the amorphous matrix is associated with the significant concentration of cobalt within its volume. The higher proportion of cobalt in this amorphous phase, compared with the amorphous matrix of the $Fe_{60}Co_{10}Y_5Zr_5B_{20}$ alloy, can be explained by the presence of crystalline phases that are rich in iron, boron and yttrium. The creation of these phases influenced the lower concentration of these elements in the amorphous phase. The second Curie temperature of 685K corresponds to the metastable magnetically-soft phase $Fe_{23}B_6$, which was identified on the basis of the X-ray diffraction pattern (fig. 1b).

Figure 4 contains magnetic hysteresis loops for the tested alloys in the post-solidification state.

The magnetic hysteresis loop measured for the $Fe_{60}Co_{10}Y_5Zr_5B_{20}$ alloy sample is typical for materials exhibiting magnetically-soft properties. In contrast, the loop measured for the$Fe_{60}Co_{10}Y_7Zr_3B_{20}$ alloy indicates clearly the presence of a magnetically-hard phase within the volume of the sample under test. The loop has an osmotic shape [30] suggesting the presence of a magnetically-hard (semi-hard) phase within the volume of the tested alloy sample. After enlarging the μ_0H-μ_0M co-ordinate system, the coercive field values for the tested samples were read. The coercive field value for the alloy with a lower Y content is 400 A/m and classifies the produced material as

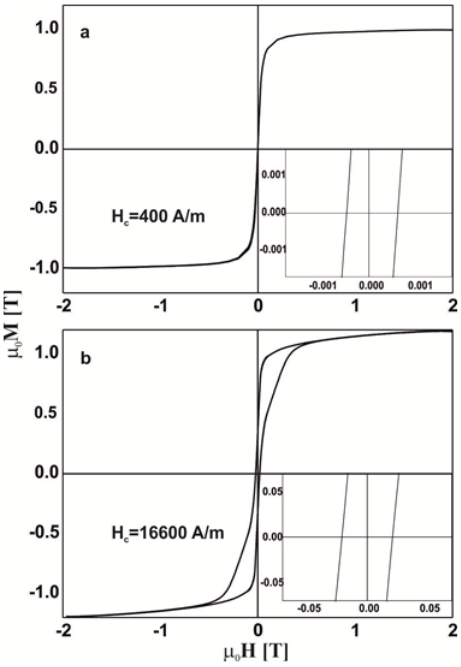

Fig.4. Hysteresis Loops for: a) $Fe_{60}Co_{10}Y_5Zr_5B_{20}$, b) $Fe_{60}Co_{10}Y_7Zr_3B_{20}$.

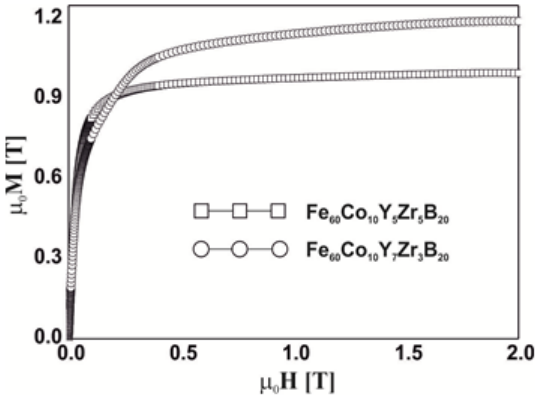

Fig. 5. Primary magnetization curves for $Fe_{60}Co_{10}Y_{5+x}Zr_{5-x}B_{20}$.

magnetically-soft. The $Fe_{60}Co_{10}Y_7Zr_3B_{20}$ alloy has a coercive field value of 16600 A/m, which can be considered magnetically-hard [31].

Figure 5 shows the primary curves of magnetization for the tested alloy samples.

The alloy sample with the lower Y content achieved a magnetization value of 1 T. The conversion of 2% atomic Zr to Y significantly affected the magnetization of saturation, yielding 1.2 T. From the course of the curves, it may be concluded that the alloy with a lower Y content is easier to magnetize and indicates the achievement of higher magnetization at lower induction of the magnetic field. The $Fe_{60}Co_{10}Y_7Zr_3B_{20}$alloy achieves a much higher value of

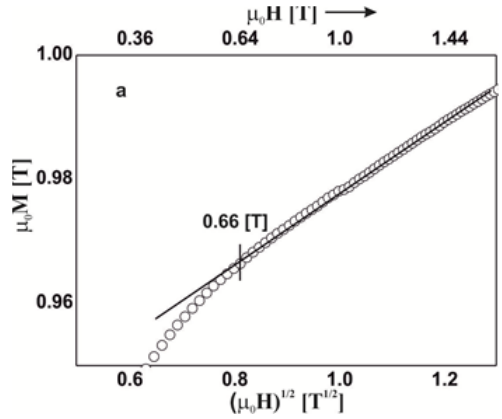

Fig. 6. High-field magnetic polarization curves, as a function of $(\mu_0 H)^{1/2}$ for: a) $Fe_{60}Co_{10}Y_5Zr_5B_{20}$,

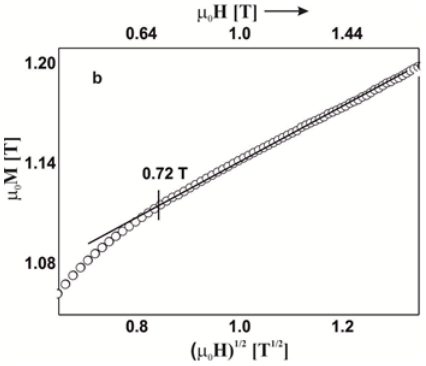

Fig. 6. High-field magnetic polarization curves, as a function of $(\mu_0 H)^{1/2}$ for: b) $Fe_{60}Co_{10}Y_7Zr_3B_{20}$.

saturation magnetization, but in the area called the approach to ferromagnetic saturation the material exerts considerable resistance against the magnetization process. This confirms the presence of a magnetically-hard phase within the volume of the alloy. Figure 6 presents the curves of 'magnetization in the area above the approach to ferromagnetic saturation', as a function of $\mu_0 M\ (\mu_0 H)^{1/2}$, for the tested alloy samples.

Significant magnetic parameters, determined for the produced alloy samples of $Fe_{60}Co_{10}Y_{5+x}Zr_{5-x}B_{20}$ are shown in table 2.

Table 2
DETERMINED MAGNETIC PROPERTIES OF THE $Fe_{60}Co_{10}Y_{5+x}Zr_{5-x}B_{20}$ alloys.

Alloy	M_s [T]	H_c [A/m]	D_{spd}[meVnm^{-2}]	T_{c1} [K]	T_{c2} [K]
$Fe_{60}Co_{10}Y_5Zr_5B_{20}$	1.00	400	45.9	538	-
$Fe_{60}Co_{10}Y_7Zr_3B_{20}$	1.20	16600	22.5	535	685

Conclusions

Massive *rapid-cooled* FeCoB alloys with rare earth alloy and other transition metal performance-enhancing additives are an interesting object of research. Slight modifications to the chemical composition of an alloy can change significantly magnetic properties such as the: coercivity field, saturation magnetization, and Curie temperature. A particularly interesting direction of research is the optimisation of chemical composition in terms of obtaining partially-crystallized alloys during the rapid-cooling of the liquid alloy. Two-phase materials, appearing in the form of nanometric crystals within the amorphous matrix, can have better magnetic properties than amorphous alloys with the same chemical composition.

The aim of this work was to produce rapid cooled alloys with high FeCoB-based and to study their structure and magnetic properties. Based on the results obtained, the following conclusions can be drawn:

-it is possible to produce single-stage materials with a fine-grained structure; i.e. during the process of rapid-cooling of the liquid alloy;

- even small changes in the chemical composition of the alloy have a significant impact on the process of atomic diffusion within the volume of the alloy, during its solidification;

- replacement of 2% atomic Y with Zr effected the formation of a magnetically semi-hard Fe_5Y phase within the volume of the alloy. The creation of this phase significantly affected the properties of the material produced. The $Fe_{60}Co_{10}Y_7Zr_3B_{20}$ alloy should be classified as magnetically-hard while the $Fe_{60}Co_{10}Y_5Zr_5B_{20}$ alloy has magnetically-soft properties;

- the higher saturation magnetization for the alloy with the higher Y content is associated with the formation of a metastable magnetic phase within the volume of the alloy: $Fe_{23}B_6$ -for which m_0M is 1.7T.

References

1.HAN,Y., WANG, Z., XU, Y., XIE Z., LI L., Journal of Non-Crystalline Solids, 442, 2016, p. 29–33.
2.WANG, W. H., DONG, C. H., Materials Science and Engineering R, 44, 2004, p. 45-89.
3.LI, W., YANG, Y. Z., XU, J., Journal of Non-Crystalline Solids, 461, 2017, p. 93–97.
4.JEZ, B., Rev. Chim (Bucharest), **68**, no. 8, 2017, p. 1903-1907.
5.ROY, R. K., PANDA, A. K., MITRA A., Journal of Magnetism and Magnetic Materials 418, 2016, p. 236–241.
6.NABIALEK, M., JEZ, K., Rev. Chim (Bucharest), **69**, no. 6, 2018, p. 1593-1597.
7.BRZOZKA, K., ŒLAWSKA-WANIEWSKA, A., NOWICKI, P., JEZUITA, K., Material Science and Engineering A, 226-228, 1997, p. 654-658.
8.INOUE, A.,YANO, N., MASUMOTO, T., J. Mater. Science, 19, 1984, p. 3786-3795.
9.SZOTA, M., Archives of Metallurgy and Materials, 62(1), 2017p. 217-222.
10.INOUE, A., ZHANG, T., MASUMOTO T., Materials Transactions JIM, 31, 1990, p. 177-183.
11.BLOCH, K., NABIALEK, M.,Acta. Phys. Pol. A, 127, 2015, p. 442–444.
12.INOUE, A., KATO, A., ZHANG, T., KIM, S.G., MASUMOTO, T., Materials Transaction JIM, 32, 1991, p. 609-616.
13.NABIA£EK, M., Arch. Metall. Mater., 61, 2016, p. 439–444.
14.IOANNOU, P.D ., NICA, P., PAUN, V., VIZUREANU, P., AGOP, M., Physica Scripta, **78**, no. 6, 2008, Article Number: 065101
15.ACHITEI, D., GALUSCA, D.G., VIZUREANU, P., CARABET, R., CIMPOESU, N., Metalurgia International, **14**, 2009, p. 45.
16.CHIRILA, E., SUSAN, M., GAVRILA, B.L., SANDU, A.V., Rev. Chim. (Bucharest), **64**, no. 5, 2013, p. 482.
17.PERJU, M.C., GALUSCA, D.G., NEJNERU, C., LARGEANU, A.E., Metalurgia International, 15, no. 11, 2010, p. 41.
18.LUCA, C., IONESCU, S.D., CHIRILA, E., Materiale Plastice, 47, no. 3, 2010, p. 370.
19.TUGUI, C.A., NEJNERU, C., GALUSCA, D.G., PERJU, M.C., AXINTE, M., CIMPOESU, N., VIZUREANU, P., Journal of Optoelectronics and Advanced Materials, 17, no. 11-12, 2015, p. 1855.
20.ACHITEI D.C., ABDULLAH, M.M.A.B., MINCIUNA, M.G., PERJU, M.C., European Journal of Materials Science and Engineering, **2**, no.4, 2017, p. 133.
21.TOTH, L., HARASZTI, F., KOVÁCS, T., European Journal of Materials Science and Engineering, **3**, no. 2, 2018, p. 98.
22.BINDEA, M., CHEZAN, C.M., PUSKAS, A., Journal Of Applied Engineering Sciences, **5**, no. 1, 2015, p. 7.
23.CIUCA, I., BOLCU, A., STANESCU, M.M., Environmental Engineering And Management Journal, **16**, no. 12, 2017, p. 2851.
24.BOLCU, D., STANESCU, M.M., CIUCA, I., MIRITOIU, C.M., BOLCU, A., CIOCOIU, R., Materiale Plastice, **54**, no. 1, 2017, p. 1.
25.MIRCEA, O., SANDU, I., VASILACHE, V., SANDU, A.V., Microscopy Research And Technique, **75**, no. 11, 2012, p. 1467.
26.KRONMÜLLER, H., FÄHNLE, M., Micromagnetism and the microstructure of ferromagnetic solids, Cambridge University Press, Cambridge 2003.
27.GRIMM, H., KRONMÜLLER, H., Physical Status Solidi B, 117, 1983, p. 663-674.
28.KRONMÜLLER, H., J. Appl. Phys., 52 (3), 1981, p. 1859 – 1864.
29.LEONOWICZ, M., Nanokrystaliczne materia³y magnetyczne, WNT, Warszawa 1998.
30.B£OCH, K., NABIA£EK, M., GARUS, S., ActaPhysicaPolonica A 130, 2016, p. 905-908.
31.LIEBERMANN H., Rapidly Solidified Alloys, Springer, New Jersey 1993.

Manuscript received: 30.08.2018